Article

Journal of
Nanoscience and Nanotechnology
Vol. 16, 9621–9633, 2016
www.aspbs.com/jnn

Catalytic Oxidation of 1,2-Propanediol to Lactic Acid with O_2 Under Atmospheric Pressure Over Pd–Ag Bimetallic Nanoparticles and Reaction Kinetics

Wuping Xue[1], Yonghai Feng[1,2], Hengbo Yin[1,*], Shuxin Liu[3], Aili Wang[1], and Lingqin Shen[1,*]

[1] *Faculty of Chemistry and Chemical Engineering, Jiangsu University, Zhenjiang, 212013, China*
[2] *School of Material Science and Engineering, Jiangsu University, Zhenjiang, 212013, China*
[3] *School of Chemistry and Chemical Engineering, Mianyang Normal University, Mianyang, 621000, China*

Catalytic oxidation of sustainable 1,2-propanediol with O_2 under atmospheric pressure to high-valued and environmentally benign lactic acid was investigated over Pd–Ag bimetallic nanoparticle catalysts. The Pd–Ag bimetallic nanoparticles were prepared by the wetness chemical reduction method with Tween as the organic modifier. The as-prepared Pd–Ag nanoparticles were characterized by XRD, HRTEM, and XPS techniques. The Pd–Ag bimetallic nanoparticles were composed of the Pd nanoparticles with the average particle sizes of 3.8–7.3 nm and the Ag nanoparticles with the average particle sizes of 15.2–30.2 nm. XRD, HRTEM and XPS analysis certified that there existed an alloy trend between Pd and Ag nanoparticles. The Pd–Ag bimetallic nanoparticles with a low Pd content effectively catalyzed the selective oxidation of 1,2-propanediol to lactic acid. When the catalytic oxidation of 1,2-propanediol with O_2 under atmospheric pressure was carried out over $Pd_{0.15}Ag_{0.85}$ nanoparticle catalyst at 85 °C for 6 h in a NaOH aqueous solution, the lactic acid selectivity was 92.8% at the 1,2-propanediol conversion of 82.7%. The kinetics for the catalytic oxidation of 1,2-propanediol over the Pd–Ag nanoparticles were affected by the Pd and Ag contents. The activation energies over Pd–Ag nanoparticles with a low Pd content were larger than those over Pd–Ag nanoparticles with a high Pd content and pure Pd nanoparticles.

Keywords: 1,2-Propanediol, Lactic Acid, Pd–Ag Bimetallic Nanoparticles, Selective Oxidation, Kinetics.

1. INTRODUCTION

By the virtue of both hydroxy and carboxylic acid groups, lactic acid can take part in many chemical reactions, such as esterification, condensation, polymerization, reduction, and substitution, which has contributed to its tremendous potential as a platform chemical for industrial production and consumer products.[1–3] In the viewpoint of green chemicals, biodegradable plastics (polylactic acid), green solvents (ethyl, propyl, butyl lactates), and oxygenated chemicals (propylene glycol) with rapid growth in market demand are produced by using lactic acid as a raw material.[4]

Lactic acid is industrially produced through either fermentation or chemical synthesis route. Fermentation process is at present the main route for lactic acid production. However, high water spending, low reaction rate, high cost of down-stream separation and purification, and biological sludge treatment are the barriers for cost-effective production of lactic acid through the fermentation process.[1] As compared to the fermentation route, the conventional chemical synthesis route through the reaction of acetaldehyde with HCN followed by hydrolysis with sulfuric acid is high selective to lactic acid with high reaction rate but is not environmentally friendly due to the use of toxic HCN.[5,6] Moreover, the chemical process using petroleum-based raw material causes high production cost.

Recently, 1,2-propanediol has been considered as an alternative raw material for the synthesis of lactic acid. 1,2-Propanediol as a biomass derivative can be facilely synthesized by catalytic hydrogenolysis of renewable glucose and polyols, such as glycerol, sorbitol, and xylitol.[7–13] Furthermore, with the scaling-up coproduction of dimethyl

---

[*] Authors to whom correspondence should be addressed.

1533-4880/2016/16/9621/013 doi:10.1166/jnn.2016.12343

carbonate and 1,2-propanediol by the transesterification method, 1,2-propanediol is facing the oversupply problem, especially in China, due to its limiting demand in the production of organic solvent and unsaturated polyester resin.[14–16] 1,2-Propanediol can be converted to lactic acid through catalytic oxidation,[5, 17–24] fermentation,[25] and electro-catalytic oxidation.[26] From among the above mentioned routes, catalytic oxidation of 1,2-propanediol to lactic acid is a more efficient and environmentally friendly route, giving high yield of lactic acid under mild reaction conditions.

Recently, selective oxidation of 1,2-propanediol to lactic acid catalyzed by Au, Pd, and Pt nanoparticles has been investigated by several research groups. In comparison with Pt and Pd, Au is more resistant to deactivation by chemical poisoning or overoxidation and displays a high intrinsic selectivity in the oxidation of 1,2-diols to 2-hydroxy-acids.[24] Thus, Au-based catalysts have received much attention in the selective oxidation of 1,2-propanediol to lactic acid.[5, 17–23] Prati et al.[5] first reported that supported gold monometallic catalyst was selective to lactic acid in catalytic oxidation of 1,2-propanediol. When the catalytic oxidation of 1,2-propanediol over 1% Au/C catalyst under 0.3 MPa O_2 at 90 °C for 1 h in an alkaline medium, the lactic acid selectivity was 78% at the complete conversion of 1,2-propanediol. Then, Xu et al.[17] reported that Au/MgO catalyst had high catalytic activity in 1,2-propanediol oxidation to lactic acid. The lactic acid selectivity was 89.3% at the 1,2-propanediol conversion of 94.4% when the oxidation reaction was carried out under 0.3 MPa of O_2 at 60 °C for 6 h. Hutchings et al.[18–20] found that when the oxidation of 1,2-propanediol was catalyzed by 0.25% Au 0.75% Pt/C catalyst under 1 MPa O_2 at 60 °C for 1 h, the lactic acid selectivity was 96% at the 1,2-propanediol conversion of 95%. However, when 1% Au/C and 1% Pt/C were used as the catalysts, the lactic acid selectivities were 67% and 96% at the 1,2-propanediol conversions of 54% and 6%, respectively. Our previous work reported that when the catalytic oxidation of 1,2-propanediol was carried out over $Au_{0.75}Pd_{0.25}/Mg(OH)_2$ catalyst at 60 °C for 4 h in a NaOH aqueous solution, the lactic acid selectivity of 88% was obtained at the 1,2-propanediol conversion of 97.5%.[22] When the catalytic oxidation of 1,2-propanediol was carried out over $Au_{0.75}Pd_{0.25}$/HAP catalyst at 80 °C for 5 h in a NaOH aqueous solution, the lactic acid selectivity was 97.1% at the 1,2-propanediol conversion of 96.6%.[23] In the supported Au–Pt and Au–Pd bimetallic catalyst, Au and Pd or Pt nanoparticles synergistically catalyzed the catalytic oxidation of 1,2-propanediol to lactic acid.[18, 21–23]

Although Ag with a low cost as compared to the noble metals, such as Au, Pd, and Pt, has good catalytic activity for various oxidation reactions, Ag–Pd bimetallic nanoparticles were seldom investigated for the oxidation of 1,2-propanediol to lactic acid. In our present work, the catalytic oxidation of 1,2-propanediol to lactic acid with O_2 to lactic acid in a NaOH aqueous solution catalyzed Ag–Pd bimetallic nanopartilces was investigated. Pd–Ag bimetallic nanoparticles were synthesized by the wetness chemical reduction method. A power function-type reaction kinetic model was used to evaluate the oxidation kinetics of 1,2-propanediol over the catalysts.

2. EXPERIMENTAL DETAILS

2.1. Materials

The chemicals, 1,2-propanediol, lactic acid, formic acid, acetic acid, hydroxyacetone, hydrazine hydrate ($N_2H_4 \cdot H_2O$), sodium hydroxide (NaOH), silver nitrate ($AgNO_3$), palladium nitrate dihydrate ($Pd(NO_3)_2 \cdot 2H_2O$), tween-80 (Tween) were of reagent grade and purchased from Sinopharm Chemical Reagent Co., Ltd. All the chemicals were used as received without further purification.

2.2. Preparation of Pd–Ag Nanoparticles

Pd_xAg_y (x, y, mole ratios of Pd and Ag to total amount of Pd and Ag) nanoparticles were prepared by the wet chemical reduction method. Typically, given amounts of silver nitrate and palladium nitrate were dissolved in 100 mL 0.05% Tween aqueous solution by ultrasonic treatment for 1 h. Then, a hydrazine hydrate aqueous solution (3.0 mL in 100 mL water) was added dropwise to the mixture at room temperature for 2 h under mild stirring. The as-prepared Pd–Ag nanoparticles were kept in an aqueous solution. The Pd–Ag nanoparticles were centrifugated and washed with anhydrous ethanol before they were characterized and used as catalysts in the oxidation of 1,2-propanediol.

2.3. Characterization

The X-ray powder diffraction (XRD) data of Pd–Ag nanoparticle catalysts were recorded on a diffractometer (D8 super speed Bruke AEX Company, Germany) using Cu Kα radiation ($\lambda = 1.54056$ Å) with Ni filter, scanning from 20° to 90° (2θ). The crystallite sizes of metallic Ag and Pd, (111) planes, were calculated by using Scherrer's equation: $D = K\lambda/(B\cos\theta)$, where K was taken as 0.89 and B was the full width of the diffraction line at half of the maximum intensity. The crystallite sizes of metallic Ag (111) and Pd (111) of the Pd–Ag nanoparticles are listed in Table I.

High-resolution transmission electron microscopy (HRTEM) images were obtained on a microscope (JEM-2100) operated at an acceleration voltage of 200 kV to characterize the morphologies and the crystal structures of Pd–Ag nanoparticles. The TEM specimens were prepared by placing a drop of Pd–Ag nanoparticles ethanol suspension onto a copper grid coated with a layer of amorphous carbon. The average particle sizes of the Pd and Ag monometallic nanoparticles were measured from the TEM images by counting at least 300 individual particles. The average particle sizes of the Pd and Ag bimetallic nanoparticles were measured from the HRTEM

Table I. Physicochemical properties of Pd–Ag nanoparticle catalysts.

	Raw materials (g)		Crystallite sizes of Ag and Pd (nm)		Average particle sizes and size distributions of Ag and Pd (nm)		Binding energies (eV)			
Catalysts	$Pd(NO_3)_2 \cdot 2H_2O$	$AgNO_3$	Ag (111)	Pd (111)	Ag	Pd	Ag $3d_{5/2}$	Ag $3d_{3/2}$	Pd $3d_{5/2}$	Pd $d_{3/2}$
Ag	0	1	32.5		38.6 13.5–67.8		368.2	374.3		
$Pd_{0.05}Ag_{0.95}$	0.08	0.95	27.7		30.2 13.7–58.2	3.8 2.3–6.5	368.1	374.1	335.0	340.3
$Pd_{0.15}Ag_{0.85}$	0.24	0.85	20.2		25.5 14.3–47.2	6 2.9–11.5	367.9	373.9	334.9	340.2
$Pd_{0.3}Ag_{0.7}$	0.47	0.7	13.3		17.4 13.2–25.9	6.6 3.5–10.9	367.4	373.4	334.7	340.0
$Pd_{0.5}Ag_{0.5}$	0.78	0.5	11.8	3.4	15.2 14.1–23.6	7.3 4.2–11.2	367.5	373.5	334.8	340.1
Pd	1	0		6.3		8.2 2.7–11.4			335.1	340.4

images by counting *ca.* 100 individual particles. The average particle sizes of Pd and Ag nanoparticles were calculated by a weighted-average method according to the individual particle sizes of the all counted particles.

X-ray photoelectron spectra (XPS) of the catalysts were recorded on an ESCALAB 250 spectrometer (PHI5000VersaProbe, UlVAC-PHI Company, Japan) using Al Kα radiation (1486.6 eV). The binding energies were calculated with respect to C1*s* peak of contaminated carbon at 284.6 eV.

2.4. Catalytic Test

The catalytic oxidation of 1,2-propanediol with O_2 was carried out in a 100-mL three-necked flask with a reflux condenser, and the flask was placed in a thermostatic bath with a magnetic stirrer. The flask was charged with the appointed amount of 1,2-propanediol, NaOH, water, and catalyst. Then, it was heated to the desired temperature, and the oxidation reaction started by bubbling O_2 with a given flow rate under stirring at 500 rpm. The reaction was monitored by sampling the reaction mixture (0.5 mL) at fixed intervals.

Before product analysis, the reaction mixture was acidified with hydrochloric acid (12 M) to the pH value of *ca*. 3. The concentration of remained 1,2-propanediol was analyzed on a gas-phase chromatograph equipped with a PEG-20 M packed capillary column (0.25 mm × 30 m) and a FID by the internal standard method with *n*-butanol as the internal standard. The products, such as lactic acid, hydroxyacetone, acetic acid, and formic acid were analyzed on a Varian HPLC system equipped with a reverse-phase column (Chromspher 5 C18, 4.6 mm × 250 mm) and a UV detector ($k = 210$ nm) at 308 K. The mobile phase was composed of H_3PO_4/NaH_2PO_4 buffer aqueous solution and acetonitrile (V:V = 9:1) with a flow rate of 0.6 mL min^{-1}. The concentrations of products were analyzed by the external standard method. The selectivities of products were calculated on carbon basis.

3. RESULTS AND DISCUSSION

3.1. XRD Analysis

The XRD patterns of Pd–Ag samples with different Ag and Pd contents are shown in Figure 1. Five XRD peaks of Ag sample appearing at $2\theta = 38.0$, 44.2, 64.3, 77.3, and 81.4° were indexed as the (111), (200), (220), (311), and (222) planes of the face centered-cubic (fcc) silver (JCPDS 04-0836), respectively. There were no other silver oxides detected by the XRD analysis, indicating that the as-prepared Ag sample was phase pure metallic Ag. The XRD peaks of Ag present in $Pd_{0.05}Ag_{0.95}$, $Pd_{0.15}Ag_{0.85}$, $Pd_{0.3}Ag_{0.7}$, and $Pd_{0.5}Ag_{0.5}$ samples appeared at $2\theta = 38.3$, 44.5, 64.7, 77.7, and 81.7°, respectively, which were *ca*. 0.4° higher than those of pure Ag sample. The XRD peaks of Pd sample appearing at $2\theta = 40.2$,

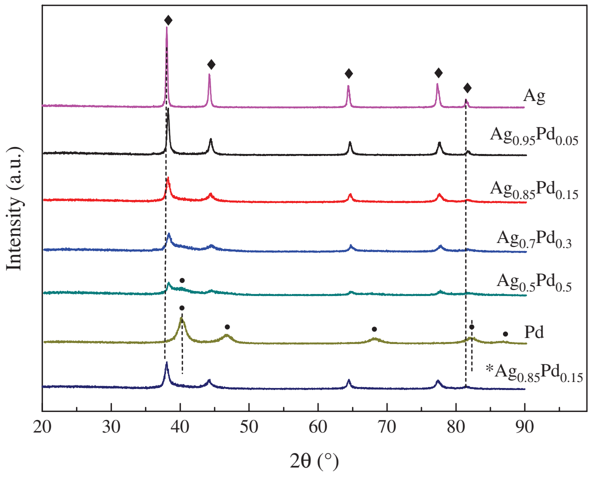

Figure 1. XRD patterns of Ag, Pd, and Pd–Ag samples. ◆, Ag; ●, Pd; ∗, spent catalyst.

46.4, 68.8, 82.0, and 87.8° were ascribed to those of the face centered-cubic (fcc) palladium (JCPDS 46-1043). There were no XRD characteristic peaks of metallic Pd detected in the XRD patterns of $Pd_{0.05}Ag_{0.95}$, $Pd_{0.15}Ag_{0.85}$, and $Pd_{0.3}Ag_{0.7}$ samples. For $Pd_{0.5}Ag_{0.5}$ sample, a weak and broad peak appearing at $2\theta = 40°$ could be indexed as the (111) plane of metallic Pd. It was *ca*. 0.2° lower than that of the pure Pd sample. As compared to the XRD peaks of pure Ag and Pd samples, the XRD peak shifts of Ag and Pd in the Pd–Ag bimetallic samples indicated that there existed an alloy trend between Pd and Ag.

The Ag (111) crystallite sizes of Ag and Pd–Ag samples were estimated by Scherrer's equation (Table I). The Ag (111) crystallite sizes were in an order of $Pd_{0.5}Ag_{0.5}$ (11.8 nm) < $Pd_{0.3}Ag_{0.7}$ (13.3 nm) < $Pd_{0.15}Ag_{0.85}$ (20.2 nm) < $Pd_{0.05}Ag_{0.95}$ (27.7 nm) < Ag (32.5 nm). The results showed that increasing the Pd content in Pd–Ag samples significantly decreased the particle sizes of Ag nanoparticles. The XRD peaks of Pd in $Pd_{0.3}Ag_{0.7}$, $Pd_{0.15}Ag_{0.85}$, and $Pd_{0.05}Ag_{0.95}$ samples were not observed, which could be ascribed to the Pd nanoparticles were well dispersed in Pd–Ag samples. When the Pd ratio was 0.5 in Pd–Ag sample, the Pd (111) crystallite size was 3.4 nm, smaller than that of the pure Pd sample (6.3 nm), indicating that increasing the Ag content in Pd–Ag samples decreased the particle sizes of Pd nanoparticles.

3.2. TEM Analysis

Figure 2 shows the TEM images of Ag, Pd, and Pd–Ag samples. The TEM image of pure Ag sample shows that the pure Ag sample was composed of Ag irregular nanoparticles with the average particle size and particle size distribution of 38.6 nm and 13.5–67.8 nm, respectively (Fig. 2(a)). Ag monometallic nanoparticles had a bimodal size distribution. The TEM image of pure Pd sample shows that the pure Pd sample was composed of small-sized Pd nanoparticles with the average particle size and particle size distribution of 8.2 nm and 2.7–11.4 nm, respectively (Fig. 2(b)).

The TEM images of Pd–Ag bimetallic samples show that the $Pd_{0.05}Ag_{0.95}$, $Pd_{0.15}Ag_{0.85}$, $Pd_{0.3}Ag_{0.7}$, and $Pd_{0.5}Ag_{0.5}$ samples were composed of Pd and Ag nanoparticles with the average particle sizes of 3.8, 30.2; 6.0, 25.5; 6.6, 17.4; 7.4, 15.2 nm, respectively (Figs. 2(c–f)). The particle sizes of Pd nanoparticles in the samples were in the order of Pd > $Pd_{0.5}Ag_{0.5}$ > $Pd_{0.15}Ag_{0.85}$ > $Pd_{0.05}Ag_{0.95}$ while the particle sizes of Ag nanoparticles were in the order of Ag > $Pd_{0.05}Ag_{0.95}$ > $Pd_{0.15}Ag_{0.85}$ > $Pd_{0.3}Ag_{0.7}$ > $Pd_{0.5}Ag_{0.5}$. The particles size distributions of Pd and Ag nanoparticles in the Pd–Ag bimetallic samples ranged from 2.3 to 11.5 and from 13.2 to 58.2 nm, respectively. The particles sizes of Pd and Ag nanoparticles in the Pd–Ag samples were significantly affected by their contents.

The TEM images show that part of small-sized Pd nanoparticles was anchored on the surfaces of large-sized Ag nanoparticles. The HRTEM image (Fig. 2(g)) also reveals that the Pd nanoparticles were anchored on the surfaces of Ag nanoparticles. However, from the TEM images, it was also found that with increasing Pd ratio in Pd–Ag bimetallic nanoparticles, the content of unanchored Pd nanoparticles increased.

The HRTEM image shows that the lattice fringes of Pd and Ag nanoparticles were examined to be *ca.* 0.228 and 0.235 nm respectively, close to the {111} lattice spacing of fcc metallic palladium and silver, respectively. It certified that metallic Pd and Ag nanoparticles were prepared under the present experimental conditions.

3.3. XPS Analysis

The XPS measurement was employed to determine the chemical states of Pd–Ag nanoparticles. The XPS spectra of Pd3*d* and Ag3*d* are shown in Figure 3 and the binding energies are listed in Table I.

The binding energies of $Ag3d_{5/2}$ and $Ag3d_{3/2}$ of pure Ag nanoparticle were 368.2 and 374.3 eV, respectively. The binding energies of $Pd3d_{5/2}$ and $Pd3d_{3/2}$ of pure Pd nanoparticles were 335.1 and 340.4 eV, respectively. The binding energies of $Ag3d_{5/2}$ and $Ag3d_{3/2}$ in the samples were in an order of Ag > $Pd_{0.05}Ag_{0.95}$ > $Pd_{0.15}Ag_{0.85}$ > $Pd_{0.3}Ag_{0.7} \approx Pd_{0.5}Ag_{0.5}$. The binding energies of Ag3*d* of Pd–Ag bimetallic nanoparticles decreased with increasing the Pd content. The binding energies of $Pd3d_{5/2}$ and $Pd3d_{3/2}$ of Pd–Ag bimetallic nanoparticles were lower than those of pure Pd nanoparticles. The binding energy shifts of Ag3*d* and Pd3*d* for Pd–Ag bimetallic nanoparticles were probably due to the alloy trend between Pd and Ag nanoparticles.

3.4. Catalytic Oxidation of 1,2-Propanediol

3.4.1. Catalytic Oxidation of 1,2-Propanediol Over Ag, Pd, and Pd–Ag Nanoparticles

The catalytic oxidation of 1,2-propanediol with O_2 under atmospheric pressure over Pd, Ag, and Pd–Ag nanoparticles was carried out in a NaOH aqueous solution at 85 °C. The results are listed in Table II.

When Ag monometallic nanoparticles were used as the catalysts, after reacting for 6 h, the 1,2-propanediol conversion was 12.8% and the selectivities of lactic acid, hydroxyacetone, formic acid, and acetic acid were 72.5%, 6.8%, 6.1%, and 14.6%, respectively. When Pd monometallic nanoparitcles were used as the catalysts, after reacting for 3 h, the 1,2-propanediol conversion was 98.2% and the selectivities of lactic acid, hydroxyacetone, formic acid, and acetic acid were 70.8%, 0%, 10.6%, and 18.6%, respectively. The Pd nanoparticles showed much higher catalytic activity in the oxidation of 1,2-propanediol than the Ag nanoparticles. Although the lactic acid selectivity over Ag nanoparticles was comparable to that over Pd nanoparticles, hydroxyacetone as an intermediate was detected over Ag nanoparticles.

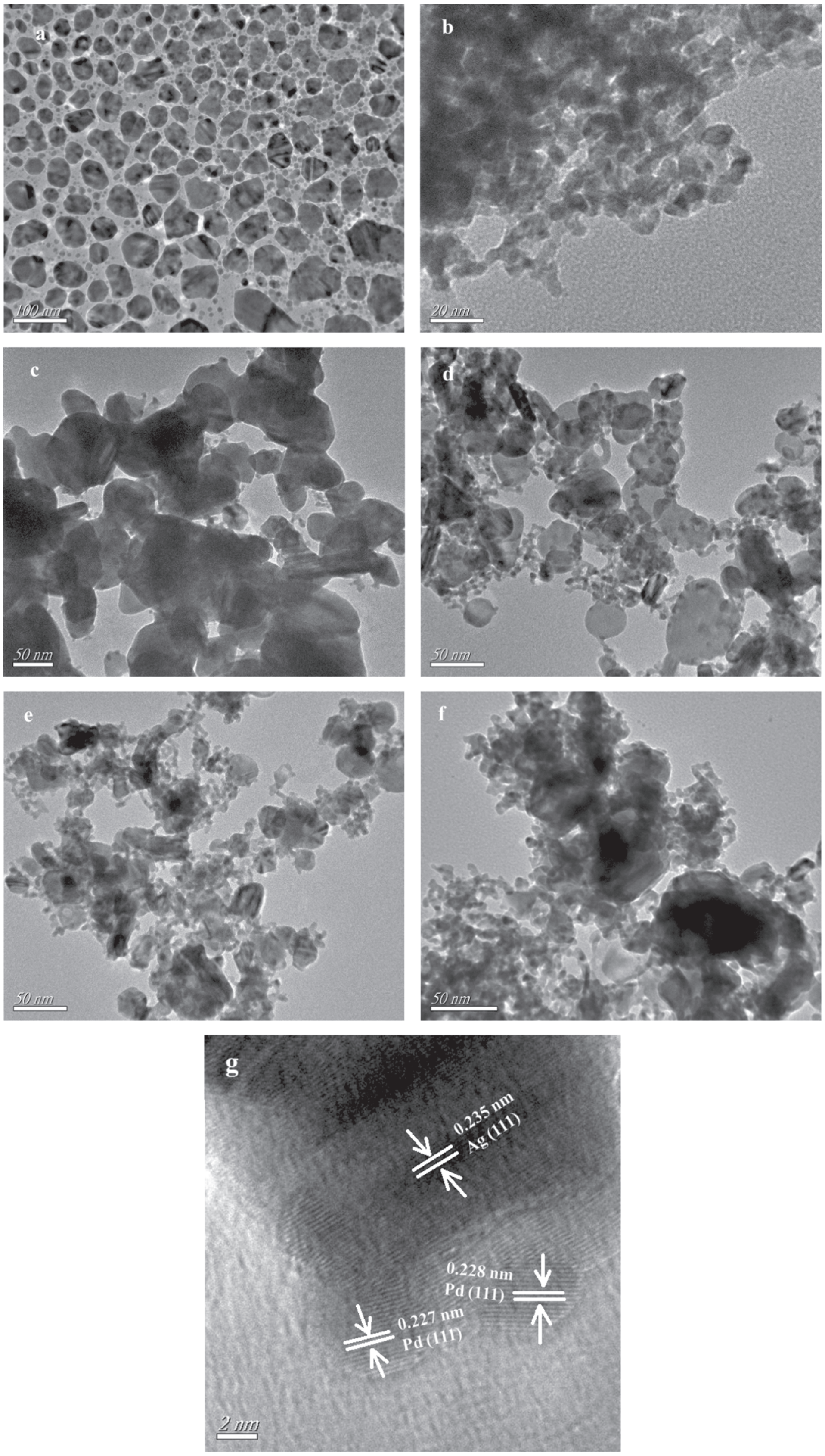

Figure 2. TEM images of (a) Ag, (b) Pd, (c) $Pd_{0.05}Ag_{0.95}$, (d) $Pd_{0.15}Ag_{0.85}$, (e) $Pd_{0.3}Ag_{0.7}$, and (f) $Pd_{0.5}Ag_{0.5}$ samples and HRTEM image of (g) $Pd_{0.15}Ag_{0.85}$ sample.

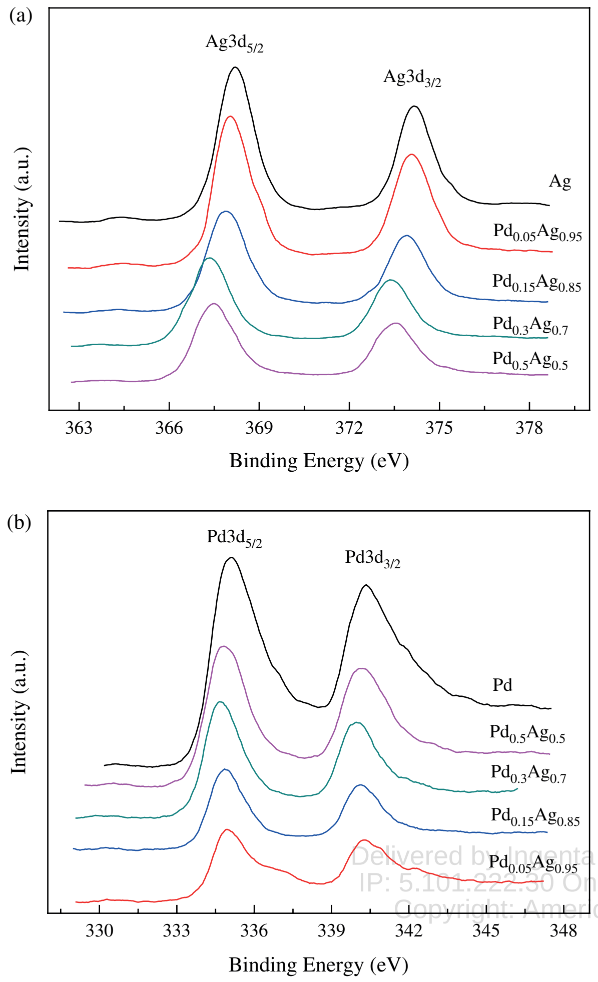

Figure 3. XPS spectra of (a) Pd3*d* and (b) Ag3*d* for the Pd–Ag nanoparticles with different Pd and Ag contents.

Table II. Catalytic oxidation of 1,2-propanediol with O_2 over Pd–Ag nanoparticles.[a]

Catalysts	Reaction times (h)	Conversions (%)	Selectivities (%) Lactic acid	Hydroxy acetone	Formic acid	Acetic acid	TOF (h^{-1})
Ag	2	4.8	73.2	7.8	5.3	13.7	1.1
	4	8.6	72.8	7.1	5.7	14.4	1.0
	6	12.8	72.5	6.8	6.1	14.6	1.0
$Pd_{0.05}Ag_{0.95}$	2	18.2	87.6	6.4	1.8	4.2	4.1
	4	31.2	87.4	5.8	2.2	4.6	3.5
	6	37.8	85.7	5.4	2.6	6.3	2.9
$Pd_{0.15}Ag_{0.85}$	2	33.2	93.7	4.1	0.7	1.5	7.5
	4	61.8	93.3	3.1	1.3	2.3	7.0
	6	82.7	92.8	2.7	1.6	2.9	6.3
$Pd_{0.3}Ag_{0.7}$	2	54.6	85.0	0	4.4	10.6	12.4
	4	88.2	78.4	0	6.4	15.2	10.0
	6	95.2	75.1	0	6.9	18.0	7.2
$Pd_{0.5}Ag_{0.5}$	2	61.3	81.2	0	6.4	12.4	13.9
	4	99.8	76.0	0	8.6	15.5	11.3
Pd	2	64.5	79.6	0	7.2	13.2	14.6
	3	98.2	70.8	0	10.6	18.6	14.8
$Pd_{0.15}Ag^{b}_{0.85}$	4	62.1	93.2	3.0	1.4	2.4	7.0

Notes: [a]Reaction conditions: 1,2-propanediol aqueous solution, 0.28 mol L^{-1}, 60 mL; NaOH concentration, 0.56 mol L^{-1}; reaction temperature, 85 °C; O_2 flow rate, 80 mL min^{-1}; catalyst loading, 0.04 g. [b]The unwashed $Pd_{0.15}Ag_{0.85}$ bimetallic nanoparticles were used as the catalysts.

When Pd–Ag bimetallic nanoparticles were used as the catalysts for the oxidation of 1,2-propanediol with O_2 under atmospheric pressure at 85 °C for 4 h, the 1,2-propanediol conversions increased from 31.2% to 99.8% with increasing the Pd ratios from 0.05 to 0.5. Maximum lactic acid selectivity of 93.3% was obtained over $Pd_{0.15}Ag_{0.85}$ catalyst. With increasing the Pd ratio to 0.3, intermediate hydroxyacetone disappeared. At high Pd contents in Pd–Ag bimetallic nanoparticles, more formic and acetic acids were formed. The results showed that the Pd–Ag bimetallic nanoparticles had high catalytic activity for the selective oxidation of 1,2-propanediol to lactic acid as compared to the Pd and Ag monometallic nanoparticles. It was interesting to find that $Pd_{0.15}Ag_{0.85}$ catalyst exhibited the highest catalytic activity for the formation of lactic acid. According to XRD analysis, there existed an alloy trend between Pd and Ag nanoparticles. Furthermore, the XPS analysis revealed that the chemical states of Pd and Ag were changed in Pd–Ag bimetallic nanoparticles as compared to the Pd and Ag monometallic nanoaprticles, respectively. It could be explained as that the alloyed Pd and Ag nanoparticles synergistically catalyzed the oxidation of 1,2-propanediol to lactic acid.[27,28] At a high Pd content, unanchored Pd nanoparticles favored the oxidation of intermediates to formic and lactic acids, acting as pure Pd nanoparticles.

To investigate the effect of the remaining organic modifier, Tween, on the catalytic activity of Pd–Ag bimetallic nanoparticles for the oxidation of 1,2-propanediol, the unwashed $Pd_{0.15}Ag_{0.85}$ bimetallic nanoparticles were used as the catalysts. Both washed and unwashed bimetallic catalysts exhibited similar catalytic activity and product selectivities (Table II). The reaction results revealed that the remaining Tween had no obvious effect on the catalytic activity of the $Pd_{0.15}Ag_{0.85}$ bimetallic nanoparticles under the present experimental conditions.

3.4.2. *Effect of Reaction Temperature*

The conversions of 1,2-propanediol and the selectivities of lactic acid, hydroxyacetone, formic acid, and acetic acid in the oxidation of 1,2-propanediol catalyzed by Pd–Ag nanoparticles at different reaction temperatures are listed in Table III. After reacting for 4 h, the conversions of 1,2-propanediol over $Pd_{0.05}Ag_{0.95}$, $Pd_{0.15}Ag_{0.85}$, and $Pd_{0.3}Ag_{0.7}$ bimetallic nanoparticles increased from 23.2% to 43.3%, 45.6% to 73.2%, and 65.7% to 94.8%, respectively, with increasing the reaction temperatures from 75 to 95 °C. After reacting for 2 h, the conversions of 1,2-propanediol over $Pd_{0.5}Ag_{0.5}$ and pure Pd nanoparticles increased from 48.4% to 79.3% and 54.6% to 87.6%, respectively, with increasing the reaction temperatures from 75 to 95 °C.

Table III. Catalytic oxidation of 1,2-propanediol with O_2 under atmospheric pressure over Pd–Ag nanoparticles at different reaction temperatures.[a]

				Selectivities (%)				
Catalysts	Temperatures (°C)	Reaction times (h)	Conversions (%)	Lactic acid	Hydroxyacetone	Formic acid	Acetic acid	TOF (h^{-1})
$Pd_{0.05}Ag_{0.95}$	75	4	23.2	86.8	8.8	1.1	3.3	2.6
	85	4	31.2	87.4	5.8	2.2	4.6	3.5
	95	4	43.3	80.8	5.4	4.4	9.4	4.9
$Pd_{0.15}Ag_{0.85}$	75	4	45.6	90.9	5.9	1.0	2.2	5.2
	85	4	61.8	93.3	3.1	1.3	2.3	7.0
	95	4	73.2	96.2	0	1.2	2.6	8.3
$Pd_{0.3}Ag_{0.7}$	75	4	65.7	88.8	3.0	2.5	5.7	7.5
	85	4	88.2	78.4	0	6.4	15.2	10.0
	95	4	94.8	76.9	0	6.6	16.5	10.8
$Pd_{0.5}Ag_{0.5}$	75	2	48.4	84.8	0	5.4	9.8	11.0
	85	2	61.3	81.2	0	6.3	12.5	13.9
	95	2	79.3	77.4	0	8.7	13.9	18.0
Pd	75	2	54.6	86.9	0	5.0	8.1	12.4
	85	2	64.5	79.6	0	7.2	13.2	14.6
	95	2	87.6	74.3	0	8.0	17.7	19.9

Note: [a]Reaction conditions: 1,2-propanediol aqueous solution, 0.28 mol L^{-1}, 60 mL; NaOH concentration, 0.56 mol L^{-1}; O_2 flow rate, 80 mL min^{-1}; catalyst loading, 0.04 g.

High reaction temperature and Pd content favored 1,2-propanediol conversion in the catalytic oxidation of 1,2-propanediol over Pd–Ag nanoparticles.

Over bimetallic Pd–Ag catalysts, the lactic acid selectivities of more than 76.9% were obtained in a reaction temperature range of 75–95 °C. The maximum lactic acid selectivity of 96.2% was obtained over $Pd_{0.15}Ag_{0.85}$ catalyst at the 1,2-propanediol conversion of 73.2%. The selectivities of hydroxyacetone decreased while the selectivities of formic and lactic acids increased with the increase in the reaction temperatures and Pd contents.

3.4.3. Effect of 1,2-Propanediol Concentration

The 1,2-propanediol conversions and product selectivities in the catalytic oxidation of 1,2-propanediol with different initial concentrations over Pd–Ag nanoparticles are listed in Table IV. The results showed that over bimetallic Pd–Ag and monometallic Pd nanoparticles, the 1,2-propanediol conversions decreased while the lactic acid selectivities increased with increasing 1,2-propanediol concentrations. The lactic acid selectivities of more than 90.5% were obtained under the initial 1,2-propanediol concentrations of 0.14–0.4 mol L^{-1} over $Pd_{0.15}Ag_{0.85}$ bimetallic catalyst.

Table IV. Catalytic oxidation of 1,2-propanediol with O_2 over Pd–Ag nanoparticles under different 1,2-propanediol concentrations.[a]

				Selectivities (%)				
Catalysts	1,2-Propanediol concentrations (mol L^{-1})	Reaction times (h)	Conversions (%)	Lactic acid	Hydroxyacetone	Formic acid	Acetic acid	TOF (h^{-1})
$Pd_{0.05}Ag_{0.95}$	0.42	4	27.9	88.6	6.3	1.5	3.5	4.7
	0.28	4	31.2	87.4	5.8	2.2	4.6	3.5
	0.14	4	45.3	82.6	4.8	4.1	8.5	2.6
$Pd_{0.15}Ag_{0.85}$	0.42	4	46.7	94.2	3.1	0.5	2.2	7.9
	0.28	4	61.8	93.3	3.1	1.3	2.3	7.0
	0.14	4	94.2	90.5	1.5	2.1	5.9	5.4
$Pd_{0.3}Ag_{0.7}$	0.42	4	68.4	90	0	3.0	7.0	11.6
	0.28	4	88.2	78.4	0	6.4	15.2	10.0
	0.14	4	98.0	72.4	0	8.7	18.9	5.6
$Pd_{0.5}Ag_{0.5}$	0.42	2	53.3	85.3	0	5.1	9.6	18.1
	0.28	2	61.3	81.2	0	6.3	12.5	13.9
	0.14	2	88.6	78.7	0	6.6	14.7	10.0
Pd	0.42	2	58.3	84.8	0	5.5	9.7	19.8
	0.28	2	64.5	79.6	0	7.2	13.2	14.6
	0.14	2	94.3	41.6	0	23.1	35.3	10.7

Note: [a]Reaction conditions: 1,2-propanediol aqueous solution, 60 mL; NaOH concentration, 0.56 mol L^{-1}; O_2 flow rate, 80 mL min^{-1}; reaction temperature, 85 °C; catalyst loading, 0.04 g.

Considering $Pd_{0.15}Ag_{0.85}$ bimetallic catalyst had high catalytic activity for the oxidation of 1,2-propanediol to lactic acid as compared to other catalysts, it was selected as the model catalyst to evaluate the effect of O_2 flow rate, NaOH concentration, and catalyst loading on the catalytic oxidation reaction in the following sections.

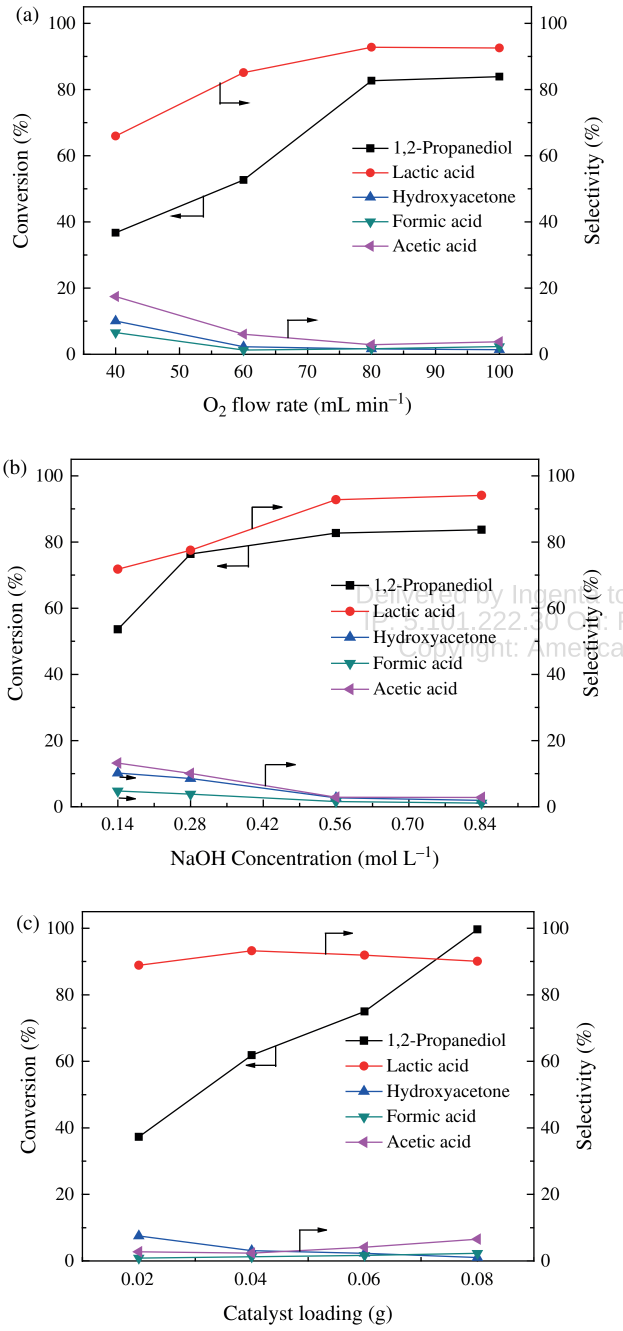

Figure 4. Effect of (a) O_2 flow rate, (b) NaOH concentration, and (c) catalyst loadings on the catalytic oxidation of 1,2-propanediol over $Pd_{0.15}Ag_{0.85}$ bimetallic nanoparticles. Except for the varied experimental parameters, the reaction condition was as follows: 1,2-Propanediol aqueous solution, 0.28 mol L^{-1}, 60 mL; NaOH concentration, 0.56 mol L^{-1}; reaction temperature, 85 °C; catalyst loading, 0.04 g, reaction time, 4 h.

3.4.4. *Effect of O_2 Flow Rate*

The 1,2-propanediol conversions and product selecticities in the catalytic oxidation of 1,2-propanediol with different O_2 flow rates over $Pd_{0.15}Ag_{0.85}$ bimetallic nanoparticles are shown in Figure 4(a). After reacting at 85 °C for 4 h, the conversions of 1,2-propanediol increased from 36.8% to 82.7% with increasing the O_2 flow rates from 40 to 80 mL min^{-1}. The selectivities of lactic acid increased from 65.9% to 92.8% while the selectivities of hydroxyacetone, formic acid and acetic acid decreased from 10.1% to 1.6%, 6.6% to 1.7%, and 17.4% to 2.9%, respectively. It demonstrated that increasing the O_2 flow rate significantly promoted the catalytic oxidation of 1,2-propanediol to lactic acid over $Pd_{0.15}Ag_{0.85}$ bimetallic nanoparticles. However, when the O_2 flow rate was raised to 100 mL min^{-1}, the conversion of 1,2-propanediol was 83.9% and the selectivities of lactic acid, hydroxyacetone, formic acid, and acetic acid were 92.5%, 1.4%, 2.3%, and 3.8%, respectively. The reaction results obtained at the O_2 flow rate of 100 min^{-1} were similar to those obtained at 80 mL min^{-1}. It could be explained as that the adsorbed O_2 on the surfaces of $Pd_{0.15}Ag_{0.85}$ nanoparticles was probably saturated at the O_2 flow rate of 80 min^{-1}. Therefore, the catalytic oxidation rate could not be significantly promoted by further increasing the O_2 flow rate.

3.4.5. *Effect of NaOH Concentration*

When 1,2-propanediol was oxidized over $Pd_{0.15}Ag_{0.85}$ bimetallic nanoparticles with the initial NaOH concentrations of 0.14, 0.28, 0.56, and 0.84 mol L^{-1}, the conversions of 1,2-propanediol were 53.6%, 76.4%, 82.7%, and 83.7%, respectively, after reacting at 85 °C for 4 h (Fig. 4(b)). The selectivities of lactic acid were 71.8%, 77.5%, 92.8%, and 94.1%. When the NaOH concentration was more

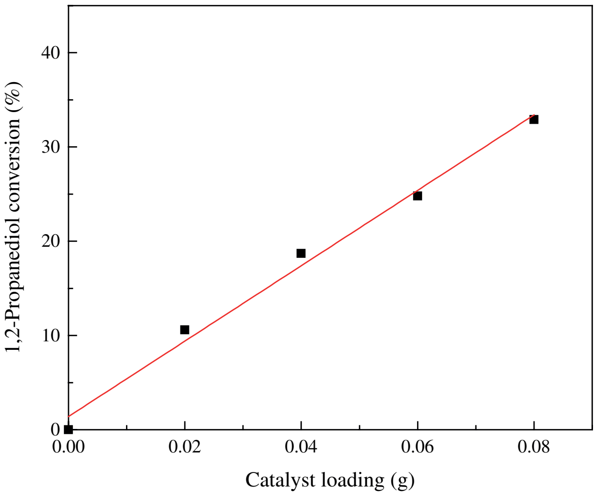

Figure 5. Catalyst loading versus 1,2-propanediol conversion. The reaction conditions: 1,2-Propanediol aqueous solution, 0.28 mol L^{-1}, 60 mL; NaOH concentration, 0.56 mol L^{-1}; reaction temperature, 85 °C; reaction time, 4 h.

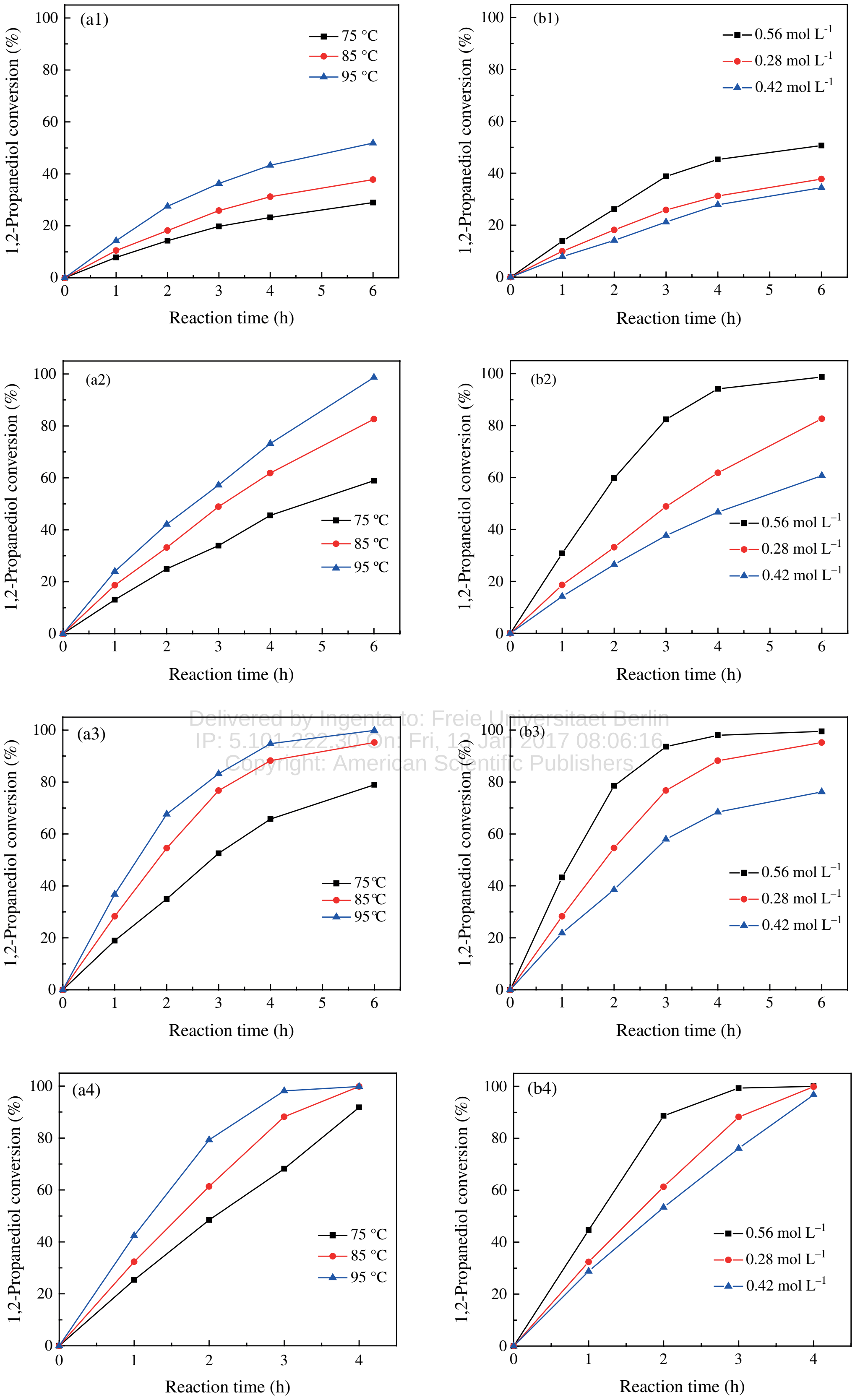

Figure 6. Continued.

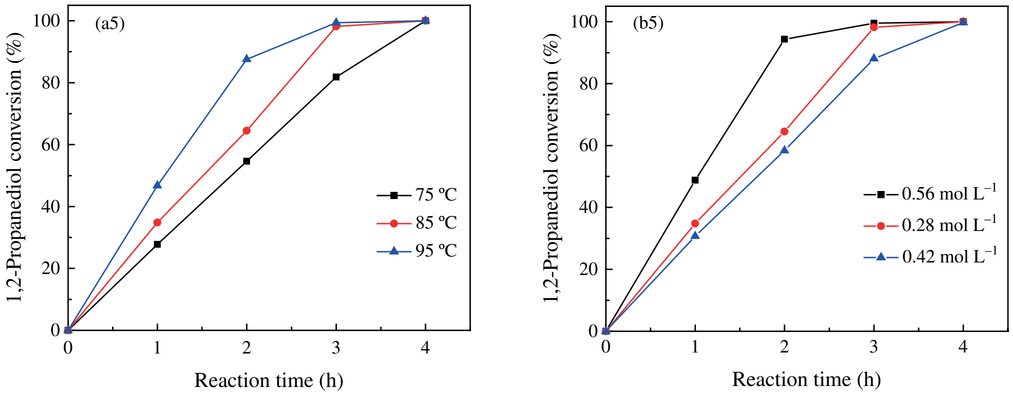

Figure 6. The conversions of 1,2-propanediol in the catalytic oxidation of 1,2-propanediol at different reaction temperatures or under different 1,2-propanediol concentrations catalyzed by (a1, b1) $Pd_{0.05}Ag_{0.95}$, (a2, b2) $Pd_{0.15}Ag_{0.85}$, (a3, b3) $Pd_{0.3}Ag_{0.7}$, (a4, b4) $Pd_{0.5}Ag_{0.5}$, and (a5, b5) Pd catalysts. Reaction conditions: (a1–4) 1,2-prapanediol aqueous solution, 0.28 mol L^{-1}, 60 mL; NaOH concentration, 0.56 mol L^{-1}; catalyst, 0.04 g; O_2 flow rate, 80 mL min^{-1}. (b1–4), 1,2-prapanediol aqueous solution, 60 mL; NaOH concentration, 0.56 mol L^{-1}; catalyst, 0.04 g; O_2 flow rate, 80 mL min^{-1}; reaction temperature, 85 °C.

than 0.56 mol L^{-1}, the total selectivies of hydroxyacetone, formic and acetic acids were less than 8%. It was found that at low NaOH concentrations, increasing NaOH concentration significantly promoted the oxidation of 1,2-propanediol to lactic acid. However, when the NaOH concentration was equal to or more than 0.56 mol L^{-1}, the oxidation of 1,2-propanediol was not obviously promoted by further increasing NaOH concentration.

3.4.6. Effect of Catalyst Loading

Figure 4(c) shows the 1,2-propanediol conversions and the product slectivities in the oxidation of 1,2-propanediol catalyzed by $Pd_{0.15}Ag_{0.85}$ bimetallic nanoparticles with different catalyst loadings. After reacting at 85 °C for 4 h, the conversions of 1,2-propanediol gradually increased from 37.3% to 99.7% with increasing the catalyst loadings from 0.02 g to 0.08 g. The selectivities of lactic acid were in a range of 88.9%–93.3%. The selectivities of hydroxyacetone decreased from 7.5% to 1.0% while the total selectivities of formic and acetic acids increased from 3.6% to 8.8%. Increasing catalyst loading obviously promoted the conversion of 1,2-propanediol to lactic acid due to more active sites available.

3.5. Reaction Kinetics

A power-function type kinetic equation was used to evaluate the effect of 1,2-propanediol concentration and reaction temperature on the reaction rate. The effect of NaOH concentration and O_2 flow rate on the reaction rate was ignored herein because the NaOH concentration and the O_2 flow rate were fixed at 0.56 mol L^{-1} and 80 mL min^{-1}, respectively. To eliminate the effect of diffusion, $Pd_{0.15}Ag_{0.85}$ catalyst with different loadings in the range of 0.02–0.12 g was used for the oxidation of 1,2-propanediol with the concentration of 0.28 mol L^{-1}. A linear correlation between the catalyst loading and the conversion was observed at first 1 h (Fig. 5). This result indicated that the initial oxidation rate was controlled only by chemical reaction rather than mass diffusion.

Taking into account of that excessive molecular oxygen was supplied in the reaction solution, it was assumed that the concentration of molecular oxygen dissolved in reaction solution was kept constant in the reaction process. The power fuction-type reaction kinetic equation can be expressed as follows.

$$r = \frac{-dC_0}{dt} = A\exp\left(\frac{-Ea}{RT}\right)C_0^n \qquad (1)$$

where C_0 is the initial 1,2-propanediol concentration, mol L^{-1}, A is the pre-exponential factor, Ea is the activation energy, kJ mol^{-1}, R is the ideal gas constant, 8.314×10^{-3} kJ mol^{-1} K^{-1}, T is the reaction temperature, K, and n is the reaction order for 1,2-propanediol concentration.

Table V. Pre-exponential factors (A), activation energies (Ea), and reaction order (n) for 1,2-propanediol over $Pd_{0.05}Ag_{0.95}$, $Pd_{0.15}Ag_{0.85}$, $Pd_{0.3}Ag_{0.7}$, $Pd_{0.5}Ag_{0.5}$, and Pd catalysts.

Catalysts	$\ln(A)$	Standard errors	A	$-Ea/R$ (10^{-3} K)	Standard errors	Ea (kJ mol^{-1})	n	Standard errors	R^2
$Pd_{0.05}Ag_{0.95}$	7.8	1.7	2438	−3.8	0.6	31.6	0.5	0.08	0.9745
$Pd_{0.15}Ag_{0.85}$	8.3	1.0	3972	−3.9	0.4	32.4	0.3	0.04	0.9865
$Pd_{0.3}Ag_{0.7}$	9.9	1.1	19622	−4.3	0.4	35.8	0.4	0.05	0.9887
$Pd_{0.5}Ag_{0.5}$	7.6	0.7	1974	−3.3	0.2	27.4	0.6	0.03	0.9962
Pd	7.7	0.7	2182	−3.3	0.3	27.4	0.6	0.04	0.9951

Linear Eq. (2) is obtained by taking the natural logarithm of both sides of the Eq. (1).

$$\ln r = \ln\left(\frac{-dC_0}{dt}\right) = \ln A - \frac{Ea}{RT} + n\ln C_0 \qquad (2)$$

To calculate the reaction order (n) and activation energy (Ea) according to Eq. (2), the initial rates were calculated according to the data shown in Figure 6. The initial reaction rates of 1,2-propanediol under different reaction conditions were calculated at the first 1 h. The values of pre-exponential factors (A), activation energies (Ea), and reaction orders (n) for 1,2-propanediol over $Pd_{0.05}Ag_{0.95}$, $Pd_{0.15}Ag_{0.85}$, $Pd_{0.3}Ag_{0.7}$, $Pd_{0.5}Ag_{0.5}$, and Pd catalysts were calculated by the multiple linear regression method (Table V).

All the experimental data gave good correlation coefficients for the power-function type kinetics in the range of 0.9745–0.9962, indicating that the power-function type kinetic model appropriated for the evaluation of the effect of 1,2-propanediol concentration and reaction temperature on the oxidation of 1,2-propanediol to lactic acid. For $Pd_{0.05}Ag_{0.95}$, $Pd_{0.15}Ag_{0.85}$, $Pd_{0.3}Ag_{0.7}$, $Pd_{0.5}Ag_{0.5}$, and Pd catalysts, their reaction kinetics were listed as follows, respectively.

$$r = \frac{-dC_0}{dt} = 2438\exp\left(\frac{-31.6}{RT}\right)C_0^{0.5} \qquad (3)$$

$$r = \frac{-dC_0}{dt} = 3972\exp\left(\frac{-32.4}{RT}\right)C_0^{0.3} \qquad (4)$$

$$r = \frac{-dC_0}{dt} = 19622\exp\left(\frac{-35.8}{RT}\right)C_0^{0.4} \qquad (5)$$

$$r = \frac{-dC_0}{dt} = 1974\exp\left(\frac{-27.4}{RT}\right)C_0^{0.6} \qquad (6)$$

$$r = \frac{-dC_0}{dt} = 2182\exp\left(\frac{-27.4}{RT}\right)C_0^{0.6} \qquad (7)$$

For $Pd_{0.05}Ag_{0.95}$, $Pd_{0.15}Ag_{0.85}$, $Pd_{0.3}Ag_{0.7}$, $Pd_{0.5}Ag_{0.5}$, and Pd catalysts, the activation energies were in an order of Ea (Pd, 27.4 kJ mol^{-1}) $= Ea$ ($Pd_{0.5}Ag_{0.5}$, 27.4 kJ mol^{-1}) $<$ Ea ($Pd_{0.05}Ag_{0.95}$, 31.6 kJ mol^{-1}) $<$ Ea ($Pd_{0.15}Ag_{0.85}$, 32.4 kJ mol^{-1}) $<$ Ea ($Pd_{0.3}Ag_{0.7}$, 35.8 kJ mol^{-1}). The activation energies were obviously affected by the contents of Pd and Ag in the Pd–Ag bimetallic catalysts. The reaction orders with respect to 1,2-propanediol concentration over $Pd_{0.05}Ag_{0.95}$, $Pd_{0.15}Ag_{0.85}$, $Pd_{0.3}Ag_{0.7}$, $Pd_{0.5}Ag_{0.5}$, and Pd catalysts were estimated to 0.5, 0.3, 0.4, 0.6, and 0.6, respectively. The $Pd_{0.15}Ag_{0.85}$ catalyst gave the lowest reaction order, indicating that the $Pd_{0.15}Ag_{0.85}$ catalyst more strongly adsorbed 1,2-propanediol than other Pd–Ag catalysts.[29] The reaction kinetics over Pd–Ag bimetallic catalysts varied with their compositions. Moreover, with increasing the Pd content in the Pd–Ag bimetallic catalyst to 0.5, the reaction kinetics over $Pd_{0.5}Ag_{0.5}$ was close to that over the Pd monometallic catalyst, indicating that at high Pd content, the Pd nanoparticles in Pd–Ag bimetallic catalyst dominantly catalyzed the oxidation reaction of 1,2-propanediol with O_2.

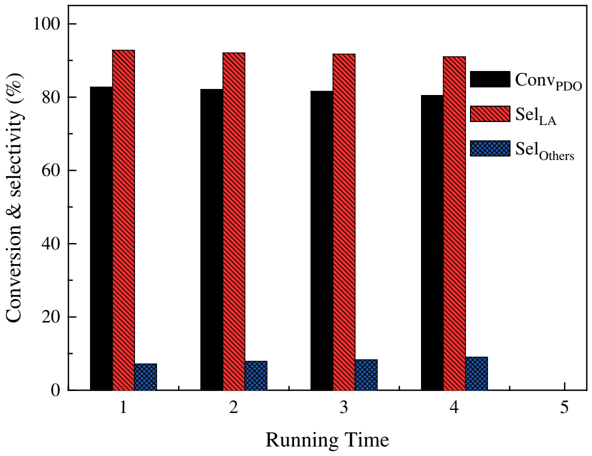

Figure 7. Recycling performance of $Pd_{0.15}Ag_{0.85}$ catalyst for the catalytic oxidation of 1,2-propanediol. Reaction conditions: 1,2-prapanediol aqueous solution, 0.28 mol L^{-1}, 60 mL; NaOH concentration, 0.56 mol L^{-1}; catalyst, 0.04 g; O_2 flow rate, 80 mL min^{-1}; reaction temperature, 85 °C; reaction time, 6 h.

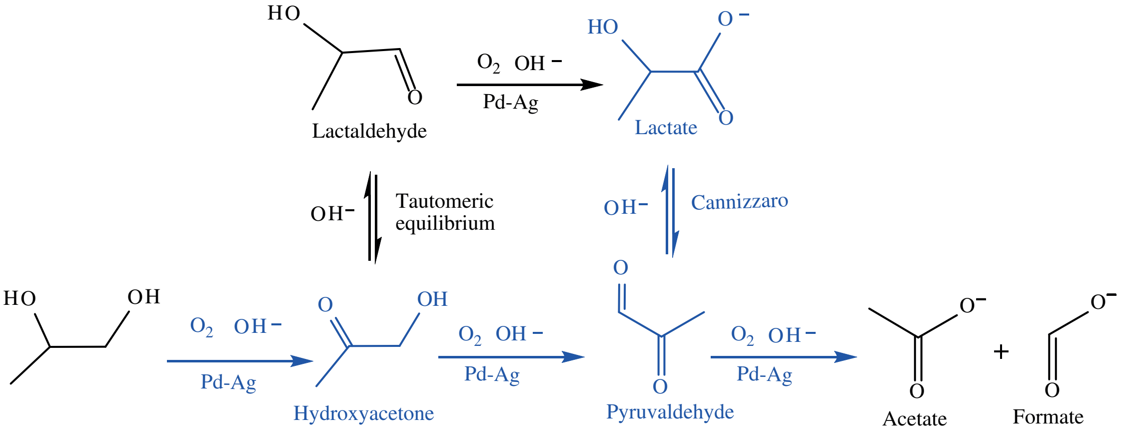

Scheme 1. Reaction routes for catalytic oxidation of 1,2-propanediol over Pd–Ag catalysts in an alkaline solution.

Table VI. Metal leaching percentages of Pd and Ag from $Pd_{0.15}Ag_{0.85}$ catalyst.[a]

				Concentrations of Pd and Ag remaining in the reaction solution		Leaching percentages of Pd and Ag	
Catalyst loading (g)	Reaction temperature (°C)	Reaction time (h)	Reaction solution (mL)	Pd ($g\ L^{-1}$)	Ag ($g\ L^{-1}$)	Pd (%)	Ag (%)
0.04	85	6	60	0.0001	0.0011	0.1	0.2

Note: [a]Reaction conditions: 1,2-prapanediol aqueous solution, 0.28 mol L^{-1}; NaOH concentration, 0.56 mol L^{-1}; O_2 flow rate, 80 mL min^{-1}. The metal leaching content in the reaction solution was measured by an atomic absorption spectrophotometry (TAS-986).

3.6. Reaction Routes

It was reported that Pd was beneficial for decreasing the coverage of strongly bound adsorbates in the catalytic oxidation of 1,2-propanediol,[21] which could be the main reason why Pd nanoparticles had high catalytic activity in the oxidation of 1,2-propanediol. However, Pd nanoparticles not only catalyzed the oxidation of 1,2-propanediol to lactic acid but also catalyzed the oxidation of intermediates to formic and acetic acids. Bimetallic Pd–Ag nanoparticle catalysts, taking $Pd_{0.15}Ag_{0.85}$ catalyst as an example, effectively catalyzed the oxidation of 1,2-propranediol to lactic acid due to the synergistic effect of alloyed Pd and Ag nanoparticles.

In the oxidation of 1,2-propanediol to lactic acid with O_2 in an alkaline solution, two reaction routes are involved as shown in Scheme 1.[17, 18, 22, 23] By the oxidation of the primary hydroxy group of 1,2-propanediol, 1,2-propanediol can be oxidized to lactaldehyde and then the resultant lactaldehyde can be rapidly oxidized to lactic acid. By the oxidation of secondary hydroxy group of 1,2-propanediol, 1,2-propanediol can be successively oxidized to hydroxyacetone and pyruvaldehyde. Pyruvaldehyde can be further oxidized to acetic acid and formic acid or converted to lactate via Cannizzaro reaction in an alkaline solution.[18] Hydroxyacetone can be transformed to lactaldehyde via the tautomeric equilibrium.

It was reported that Pd–Ag alloy catalysts favored the oxidation of the secondary OH group of *vic*-diols.[29] Furthermore, hydroxyacetone was detected in the catalytic oxidation of 1,2-propanediol over Pd–Ag bimetallic nanoparticles with O_2 in an alkaline solution. The selectivity of hydroxyacetone decreased with increasing the catalytic activity of catalyst and prolonging the reaction time. The result indicated that hydroxyacetone was an intermediate in the oxidation of 1,2-propanediol over Pd–Ag bimetallic nanoparticles. Therefore, it was reasonable to conclude that the formation of lactic acid in the catalytic oxidation of 1,2-propanediol with O_2 over Pd–Ag bimetallic nanoparticles in an alkaline solution was mainly through the oxidation of secondary hydroxy group of 1,2-propanediol.

3.7. Recycling Performance

The recycling performances of $Pd_{0.15}Ag_{0.85}$ catalyst for the oxidation of 1,2-propanediol are shown in Figure 7. After reacting at 85 °C for 6 h, the used catalyst was centrifugated and washed with anhydrous ethanol before next recycling. As shown in Figure 7, the conversion of 1,2-propanediol and the selectivity of lactic acid over the fresh $Pd_{0.15}Ag_{0.85}$ catalyst were 82.7% and 92.8%, respectively. After running for 4 times, the conversion of 1,2-propanediol and the selectivity of lactic acid over $Pd_{0.15}Ag_{0.85}$ catalyst were 80.4% and 91.0%, respectively. The XRD pattern of the spent catalyst was the same as that of the fresh one (Fig. 1). After reacting at 85 °C for 6 h, the metal leaching percentages of Pd and Ag from the bimetallic catalyst were 0.1% and 0.2% (Table VI), respectively. The results revealed that the Pd–Ag nanoparticle catalyst had good recycling performance.

4. CONCLUSIONS

Pd–Ag bimetallic nanoparticles were prepared by the wet chemical reduction method. The average particle sizes of Pd and Ag nanoparticles were in the ranges of 3.8–7.3 nm and 15.2–30.2 nm, respectively, which were significantly affected by the contents of Pd and Ag. XRD, HRTEM, and XPS analysis showed that there was an alloy trend between Pd and Ag nanoparticles in Pd–Ag bimetallic nanoparticles. Pd–Ag bimetallic nanoparticles with low Pd content effectively catalyzed the selective oxidation of 1,2-propanediol to lactic acid. However with high Pd content, the catalytic activity of Pd–Ag nanopaticles for the oxidation of propanediol was the same as that over pure Pd nanoparticles.

When the catalytic oxidation of 1,2-propanediol with O_2 under atmospheric pressure was carried out over $Pd_{0.15}Ag_{0.85}$ nanoparticles at 85 °C for 6 h in an alkaline solution, the lactic acid selectivity was 92.8% at the 1,2-propanediol conversion of 82.7%.

The kinetics for the catalytic oxidation of 1,2-propanediol over Pd–Ag bimetallic nanoparticles were affected by their compositions. The activation energies over Pd–Ag nanoparticles with a low Pd content were larger than those over Pd–Ag nanoparticles with a high Pd content and pure Pd nanoparticles.

Acknowledgments: The authors sincerely thank Professor K. Chen (Jiangsu University) for supporting the TEM and HRTEM measurements. This work was financially supported by research funds from Jiangsu Province Education Bureau (Nos. 11KJB530002 and 1102120C), Jiangsu University for Young Researchers (Nos. 11JDG028, 2010-4849, and 15JDG026), China Postdoctoral Foundation Committee (No. 2011M500866) and Ph.D. Innovation Programs Foundation of Jiangsu Province (No. CXZZ13_0666).

References and Notes

1. P. Pal, J. Sikder, S. Roy, and L. Giorno, *Chem. Eng. Process.* 48, 1549 (**2009**).
2. A. Babu, J. Periasamy, A. Gunasekaran, G. Kumaresan, S. Naicker, P. Gunasekaran, and R. Murugesan, *J. Biomed. Nanotechnol.* 9, 177 (**2013**).
3. P. Pradhan, B. K. Poudel, T. Ramasamy, H. G. Choi, C. S. Yong, and J. O. Kim, *J. Nanosci. Nanotechnol.* 13, 5948 (**2013**).
4. R. Datta and M. Henry, *J. Chem. Technol. Biotechnol.* 81, 1119 (**2006**).
5. L. Prati and M. Rossi, *J. Catal.* 176, 552 (**1998**).
6. N. Narayanan, P. K. Roychoudhury, and A. Srivastava, *Microb. Biotechnol.* 7, 1 (**2004**).
7. Y. Feng, H. Yin, L. Shen, A. Wang, Y. Shen, and T. Jiang, *Chem. Eng. Tech.* 36, 73 (**2013**).
8. R. M. Williams and J. W. Medlin, *Surf. Sci.* 619, 30 (**2014**).
9. D. Liang, C. Liu, S. Deng, Y. Zhu, and C. Lv, *Catal. Commun.* 54, 108 (**2014**).
10. Y. Feng, H. Yin, A. Wang, L. Shen, L. Yu, and T. Jiang, *Chem. Eng. J.* 168, 403 (**2011**).
11. A. Bienholz, H. Hofmann, and P. Claus, *Appl. Catal. A: Gen.* 391, 153 (**2011**).
12. L. Zhao, J. H. Zhou, Z. J. Sui, and X. G. Zhou, *Chem. Eng. Sci.* 65, 30 (**2010**).
13. C. Montassier, J. C. Ménézo, L. C. Hoang, C. Renaud, and J. Barbier, *J. Mol. Catal.* 70, 99 (**1991**).
14. B. M. Bhanage, S. Fujita, Y. Ikushima, and M. Arai, *Green Chem.* 5, 429 (**2003**).
15. http://www.docin.com/p-445508830.html.
16. http://mcgroup.co.uk/news/20140418/propylene-glycol-market-reach-supplydemand-balance-2015.html.
17. H. Ma, X. Nie, J. Cai, C. Chen, J. Gao, H. Miao, and J. Xu, *Sic. China Chem.* 53, 1497 (**2010**).
18. N. Dimitratos, J. A. Lopez-Sanchez, S. Meenakshisundaram, J. M. Anthonykutty, G. Brett, A. F. Carley, S. H. Taylor, D. W. Knighta, and G. J. Hutchings, *Green Chem.* 11, 1209 (**2009**).
19. Y. Ryabenkova, P. J. Miedziak, N. F. Dummer, S. H. Taylor, N. Dimitratos, D. J. Willock, D. Bethell, D. W. Knight, and G. J. Hutchings, *Top. Catal.* 55, 1283 (**2012**).
20. Y. Ryabenkova, Q. He, P. J. Miedziak, N. F. Dummer, S. H. Taylor, A. F. Carley, D. J. Morgan, N. Dimitratos, D. J. Willock, D. Bethell, D. W. Knight, D. Chadwick, C. J. Kiely, and G. J. Hutchings, *Catal. Today* 203, 139 (**2013**).
21. M. B. Griffin, A. A. Rodriguez, M. M. Montemore, J. R. Monnier, C. T. Williams, and J. W. Medlin, *J. Catal.* 307, 111 (**2013**).
22. Y. Feng, H. Yin, A. Wang, D. Gao, X. Zhu, L. Shen, and M. Meng, *Appl. Catal. A: Gen.* 482, 49 (**2014**).
23. Y. Feng, H. Yin, D. Gao, A. Wang, L. Shen, and M. Meng, *J. Catal.* 316, 67 (**2014**).
24. P. G. N. Mertens, M. Bulut, L. E. M. Gevers, I. F. J. Vankelecom, P. A. Jacobs, and D. E. De Vos, *Catal. Lett.* 102, 57 (**2005**).
25. W. Su, Z. Y. Chang, K. L. Gao, and D. Z. Wei, *Tetrahedron: Asymmetry.* 15, 1275 (**2004**).
26. M. M. Dimos and G. J. Blanchard, *J. Electroanal. Chem.* 654, 13 (**2011**).
27. F. Mauriello, H. Ariga, M. G. Musolino, R. Pietropaolo, S. Takakusagi, and K. Asakura, *Appl. Catal. B.* 166-167, 121 (**2015**).
28. D. Tongsakul, S. Nishimura, and K. Ebitani, *ACS Catal.* 3, 2199 (**2013**).
29. S. Hirasawa, H. Watanabe, T. Kizuka, Y. Nakagawa, and K. Tomishige, *J. Catal.* 300, 205 (**2013**).

Received: 16 July 2015. Accepted: 11 August 2015.